Proceedings of IDETC/CIE 2005
ASME 2005 International Design Engineering Technical Conferences
& Computers and Information in Engineering Conference
September 24-28, 2005, Long Beach, California USA

DETC2005-84821

THREE DIMENSIONAL CALCULATION OF MESHING STIFFNESS FOR SPUR GEARS

Mohammad Durali
Mechanical Engineering Department
Sharif University of Technology
PO Box 11365-9567, Tehran Iran
durali@sharif.edu

Mariam Gh. Saryazdi
Mechanical Engineering Department
Sharif University of Technology
PO Box 11365-9567, Tehran Iran
saryazdi@mehr.sharif.edu

ABSTRACT

This article presents a new method for determination of meshing stiffness of the gear teeth using three dimensional analysis of tooth stiffness. The teeth are treated as explicit capacitive fields and their compliance matrix is determined by considering virtual interconnected springs located at defined nodes on tooth profile. The stiffness of any arbitrary point on the profile can then be determined as a linear function of neighboring nodes stiffness. The results of this analysis help in determination of load distribution for a pair of meshing gears under real operation conditions where deflections and misalignments are inevitable.

INTRODUCTION

Gear boxes are among most important elements of mechanical systems, and their maintenance and condition monitoring are of prime concern to users and service personal. Torsional vibrations of gears and shafts are more important in gearbox performance than their lateral and longitudinal vibrations because they directly affect the quality of power transmission. Therefore many efforts have been put into monitoring gearbox working condition by noise and vibration measurement on gearboxes by different methods.

The main source of gear torsional vibrations is the change in meshing stiffness. Meshing stiffness changes periodically as contact point changes position over the tooth profile. This will induce periodic changes in gear loading. Local defects such as crack or tooth fracture also change meshing stiffness increasing vibration amplitudes. Therefore a correct measurement of meshing stiffness and its changes can help in better understanding of induced vibrations and resulting defects.

There has been many works on calculation of tooth stiffness. These works mainly use analytical, experimental, or numerical methods for this calculation. In early works by Tuplin and Buckingham meshing stiffness was considered to be constant [3]. Later work considered meshing stiffness as a periodic function. Dalpiaz [1], considered a sine shape and Seireg [5], a trapezoidal shape for this periodic function. Shing [6] used theory of elasticity to determine the mean meshing stiffness. He considered deflection contributed by bending moment and shear stress, foundation deflection and Hertzian stress as the main parameters affecting tooth deflection. Kuang [3] used a two dimensional (2-D) finite element method (FEM) to calculate tooth stiffness. He expressed the tooth stiffness as a function of module, number of teeth, pitch circle diameter, and the position of contact point. Yesilyurt [9] used experimental results and modal analysis to calculate meshing stiffness. Pimsarn [4] defined the singular stiffness at the contact point of the bodies and calculated the contact force on the basis of artificial overlap of two rigid bodies. His calculation scheme was 2000 times faster than a FEM calculation for the same problem but had 8% difference with FEM results.

In all previous analytical or numerical studies on gear meshing, a two dimensional model has been considered. However, there are many factors in real working condition that divert the line of contact from its ideal position. Gear shaft deformation, deformations of the housing, shaft misalignment, bearing deformations and imperfections, and elastic deformations of gear body are among these parameters [2].

In the current research a method is devised by which meshing stiffness is calculated using the results of 3-D FEM analysis of gear tooth. The gear tooth is treated as a capacitive field and its compliance matrix is determined. This will give a new capability for analyzing gear tooth loading in three dimensional loading situations resulting from real working conditions.

A REVIEW OF 2-D MODELS

Figure 1 shows a two dimensional model of a pair of meshing gears. In this model it is assumed that the line of contact of the two gears is parallel to the axes of the gears, and the meshing is modeled as a spring and damper. The frictional effects are normally ignored in this model.

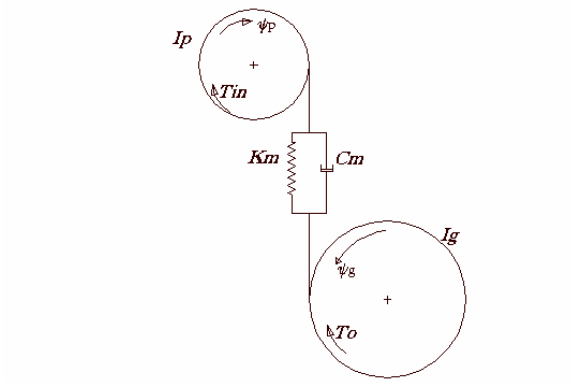

Figure 1- two dimensional model of a pair of meshing gears.

In Fig.1, T represents torque, I is the moment of inertia, K_m is meshing stiffness, and C_m is the meshing damping. The meshing force F resulting from material elasticity is related to the relative displacement of the two gears as represented in Equation 1.

$$F = K_m\left(\rho_p\psi_p - \rho_g\psi_g\right) \tag{1}$$

In Equation 1, ρ is the radius of contact point. To calculate meshing stiffness, the stiffness of a single tooth must be determined. Let's define the tooth stiffness as the ratio of the force applied to the tooth to the displacement in direction of the force:

$$K = \frac{F}{\delta} \tag{2}$$

Meshing stiffness is a function of tooth form, contact ratio, radii of profile curvature, the rim section design, the Hertz contact, manufacturing errors, elasto-hydrodynamic lubrication and the alignment errors [6]. The meshing stiffness is calculated from single tooth stiffness as springs in series [6]:

$$K_m = \frac{1}{K_1} + \frac{1}{K_2} \tag{3}$$

If more than one pair of teeth comes to contact at the same time, the meshing stiffness becomes:

$$K = K_{m1} + K_{m2} + ... \tag{4}$$

Meshing stiffness is a periodic function and changes with gears rotating position. If the spring constant of a single tooth as a function of contact point is known, the meshing stiffness can be determined at each working moment.

THE3- D MODEL

In real working conditions, many factors dislocate the line of contact from its ideal position and therefore the two dimensional model of meshing stiffness can no longer be used. Determination of meshing stiffness using 3-D models is very time consuming and not feasible. The method presented in this article uses the results of the finite element analysis done on a 3-D model of the gear for this purpose. In this method the volume of the calculations are reduced remarkably.

Each tooth in this model is assumed to have numerous compression springs on its surface. During meshing, n springs from pinion tooth, lined on the line of contact (K_{pi}), push on n springs on the gear tooth (K_{gi}). The assumed springs on the pinion tooth constitute a capacitive field whose stiffness matrix $[K_p]$ is determined by 3-D finite element analysis. Likewise a stiffness matrix is determined for gear teeth $[K_g]$. These capacitive fields are functions of the position of contact line and their elements change as the line of contact changes position due to motion.

The Capacitive Fields

Each gear tooth surface is divided to a large enough number of regions to provide the required accuracy (circles in Fig. 2). A unit load is then applied to each of the nodes and the tooth is analyzed to find the displacement of the nodes on the tooth surface. Repeating this for all the nodes on the tooth will result a displacement matrix u whose elements u_{ij} are the displacement in node i as a result of a unit load at node j. The matrix u will then be used as a reference to calculate the meshing stiffness.

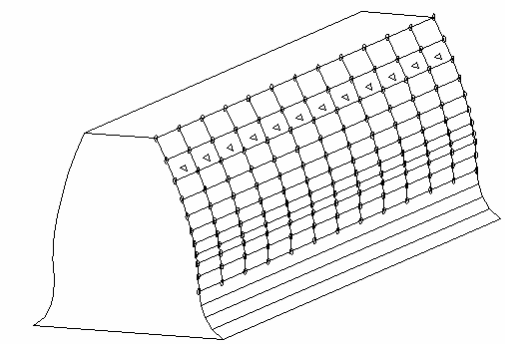

Figure 2- FEM node positions on the tooth (dots), points on line of contact (triangles).

If load is applied to nodes 1 to n simultaneously, the displacement of a node can be determined by linear superposition of the displacements of that node due to the applied loads. Using this terminology, the displacement of node 1 on can be defined as:

$$U_1 = f_1u_{11} + f_2u_{12} + ... + f_nu_{1n} \tag{5}$$

Similarly for i^{th} node we have:

$$U_i = f_1u_{i1} + f_2u_{i2} + ... + f_nu_{in} \tag{6}$$

And in matrix form:

$$\{U\} = [u]\{f\} \tag{7}$$

It is apparent that u is the compliance matrix of the tooth and its inverse will therefore be the tooth stiffness matrix.

$$[K] = [u]^{-1} \tag{8}$$

The stiffness matrix K is determined by the assumption that the loads are applied at the nodes. In real working condition the line of contact can have different positions and its points are not necessarily on the nodes. Matrix u can be used to determine the displacement of any other point not lying on the nodes. As shown in fig, 2, the points marked by triangles are assumed to be the points on an arbitrary line of contact. Each of these points is located between four nodes. The displacements of these points due to the force applied at nodes can be determined by a linear shape function. Considering C^0 continuity we have [7]:

$$u_n = c_1 + c_2x + c_3y + c_4xy \tag{9}$$

In Equ. 9, c_is are constants and x and y denoted the position of the point of interest. As u_i is known in nodes 1 to 4 (for example), the coefficients c_i can be determined using Equation 10 [7]:

$$\begin{bmatrix} c_1 \\ c_2 \\ c_3 \\ c_4 \end{bmatrix} = \begin{bmatrix} 1 & x_1 & y_1 & x_1 y_1 \\ 1 & x_2 & y_2 & x_2 y_2 \\ 1 & x_3 & y_3 & x_3 y_3 \\ 1 & x_4 & y_4 & x_4 y_4 \end{bmatrix} \begin{bmatrix} u_1 \\ u_2 \\ u_3 \\ u_4 \end{bmatrix} \tag{10}$$

This can be done for other points on a line of contact and not on the nodes. As next step Castigliano's theorem, can be used to determine the displacement of the new points as a result of the application of the load to the same points and therefore the new displacement matrix [u] can be determined from Equ. 7.

3-D Meshing Stiffness

If the line of contact is known, the corresponding capacitive field associated with that can be determined using the method described before. The assumed springs on the surface of the two teeth will be in series on the line of contact. If u_p represent displacement of the pinion tooth, u_g displacement of gear tooth, and u_c the displacement on the line of contact, then:

$$\{F\} = [K_p]\{u_p - u_c\} \tag{11}$$

And similarly:

$$\{F\} = [K_g]\{u_c - u_g\} \tag{12}$$

In the above equations F is a $1xn$ matrix representing the force on the points along the line of contact and K_p and K_g are stiffness matrices of the pinion and the gear respectively (note that stiffness matrices are functions of the line of contact and vary with gears rotation). The displacements of the line of contact can be determined from equations 11 and 12:

$$\{u_c\} = [C_{pg}]\left([K_p]\{u_p\} + [K_g]\{u_g\}\right) \tag{13}$$

In which

$$[C_{pg}] = \left([K_p] + [K_g]\right)^{-1} \tag{14}$$

As a result the meshing force as a function of pinion and gear displacements will be:

$$\begin{aligned} \{F\} &= [K_g][C_{pg}][K_p]\{u_p\} \\ &+ [K_g]\left([C_{pg}][K_g] - [I]\right)\{u_g\} \end{aligned} \tag{15}$$

The displacement of pinion and gear teeth are related to the corresponding rotation angles as follows:

$$\{u_p\} = \{R_{pc}\}\theta_p \tag{16}$$

$$\{u_g\} = \{R_{gc}\}\theta_g \tag{17}$$

In above equations, R_{pc} and R_{gc} are the radii of rotations of pinion and gear teeth contact points. The radius of rotation changes along tooth profile, and it can be related to the tooth and gear geometry. The changes are not large and at this stage it will only add to the complexity of the relations. We preferred to use the pitch radius of the gears instead in a trade for simplicity. It will then result:

$$\begin{aligned} \{F\} &= [K_g][C_{pg}][K_p]\{R_{pc}\}\theta_p \\ &- [K_g]\left([I] - [C_{pg}][K_g]\right)\{R_{gc}\}\theta_g \end{aligned} \tag{18}$$

The problem is symmetric by nature and therefore the stiffness matrix can be achieved:

$$[K_g][C_{pg}][K_p] = [K_g]\left([I] - [C_{pg}][K_g]\right) \tag{19}$$

Substituting equation 18 into 19 results:

$$\{F\} = [K_g][C_{pg}][K_p]\left(\{R_{pc}\}\theta_p - \{R_{gc}\}\theta_g\right) \tag{20}$$

For a unit relative displacement we have:

$$\{R_{pc}\}\theta_p - \{R_{gc}\}\theta_g = 1 \tag{21}$$

And for a unit relative displacement the meshing force of the two gears will be the meshing stiffness:

$$\{K_m\}_{n\times 1} = \left([K_g][C_{pg}][K_p]\right)_{n\times n}\{1\}_{n\times 1} \tag{22}$$

Figure 3 shows the schematic of the meshing configuration.

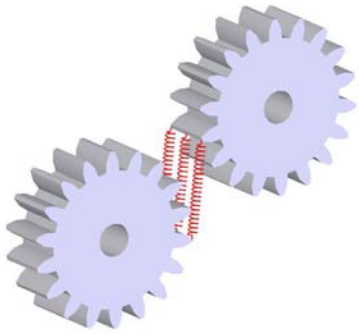

Figure 3- Schematics of 3-D meshing configuration on the line of contact.

This will constitute a discrete structural with an explicit capacitive field as shown in figure 4 in a Bond Graph representation. In this figure R_{ci} is the radius of the meshing point and K_{mi} is the equivalent spring constant of that point.

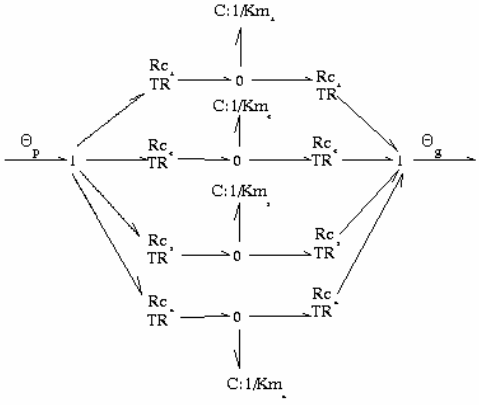

Figure 4- Bond Graph representation of meshing stiffness.

APPLICATION TO AN EXAMPLE

For a gear tooth whose specifications are given in table1, the application of this approach is illustrated. A tooth from this gear is modeled in a 3-D manner using the relation presented by Litvin [3]. The generated geometric model of this gear was meshed using hexagonal elements. There are 91 nodes on the surface of this tooth arranged in 7 rows of 13 nodes each. In each round of calculation a normal force is applied to each one of these nodes and the case was analyzed using FEM calculations to obtain the displacement of all the nodes due to applied load. The calculation was repeated for all the nodes until completed. In the next step using the results of FEM calculations, the compliance matrix u and from that and equation 22, the stiffness matrix of the gear was obtained.

Table 1- specifications of the gear under study

Gear Module	3
Number of Teeth	20
Pressure Angle	20^o
Helix Angle	0^o
Face Width	24 mm

Comparison of the2-D and 3-D results

Kung used a 2-D model for determination of meshing stiffness, and changing module, number of teeth, and addendum modification coefficient, he calculated the gear stiffness for four points on the profile i.e. the initial contact point (IP), the highest point of single tooth contact (HPSTC), the lowest point of single tooth contact (LPSTC), and the final contact point (FP). The function describing the tooth stiffness as a function of tooth specifications is presented in equation 23 [3].

$$K_i(r_i) = (A_0 + A_1 X_i) + (A_2 + A_3 X_i)\frac{r_i - R_i}{(1+X_i)m} \quad N/\mu m/mm \tag{23}$$

In Equ. 23, R_i, X_i, and N_i are pitch radius, addendum correction factor, and number of teeth of the i^{th} gear. The constants ($A_i s$), are determined by the relations given in Equation 24 [3].

$$\begin{aligned} A_0 &= 3.867 + 1.612N_i - .02916N_i^2 + .0001553N_i^3 \\ A_1 &= 17.060 + 0.7289N_i - .01728N_i^2 + .0000993N_i^3 \\ A_2 &= 2.637 - 1.222N_i + .02217N_i^2 - .0001179N_i^3 \\ A_3 &= -6.330 - 1.033N_i - .02068N_i^2 - .0001130N_i^3 \end{aligned} \tag{24}$$

For the four points mentioned above, meshing stiffness was calculated using equation 23. The meshing gears were considered to equal and having the specifications listed in table 1. Also meshing stiffness was calculated for the same points based on 3-D model and using equation 22. In both cases the meshing is considered to be ideal and across full face, the gear axes are parallel, and that the line of contact stays parallel to the axes of the gears. Figure 5 compares the results. Also the numeric values of the two approaches are listed in table 2. The difference in meshing stiffness between 2-D and 3-D models for this case is about 4%.

Table 2- Comparison of meshing stiffness calculated from 2-D and 3-D models

Contact point	2D FEM	New Method	Error
IP	3.5043	3.3716	3.8%
HPSTC	5.0414	5.2516	4.2%
LPSTC	5.0414	5.2516	4.2%
FP	3.5043	3.3716	3.8%

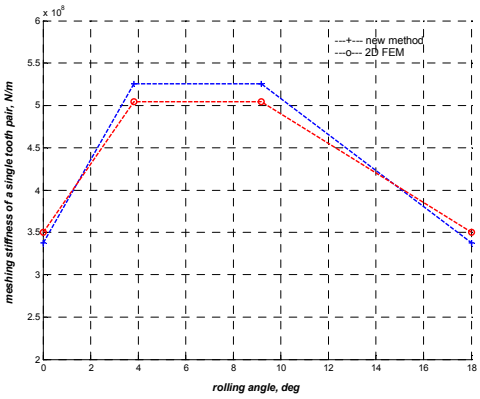

Figure 5- Meshing stiffness calculated from 2-D FEM and the new method.

VARIATION OF MESHING STIFFNESS IN IDEAL MESHING

When gears have parallel axes, the line of contact will be parallel with the gear axes and gear loading is symmetrical across the face. For such case meshing stiffness was calculated for 13 points of equal distance along the line of contact. The load is applied at the four points study point namely IP, HPSTC, LPSTC, and FP. Figure 6 shows the variation of meshing stiffness as a function of rotation angle, for a pair of meshing gears introduced in table 1, in three points along the tooth width. As expected, the edges of the teeth seem to be less stiff and as we approach the center of the tooth, the meshing stiffness reaches a peak.

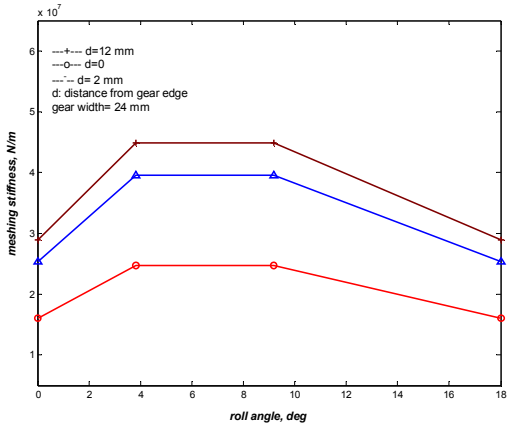

Figure 6- Variation of meshing stiffness as a function of rotation angle in three points along tooth width

Figure 7 shows the variations of meshing stiffness as a function of gear width for two positions along the tooth profile, namely HPSTC and IP.

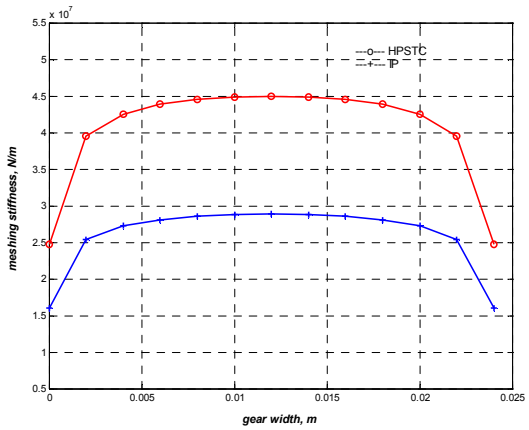

Figure 7- Meshing stiffness variation with gear width for two positions along the tooth profile.

THE EFFECT OF SHAFT MISALIGNMENT

If the shafts of the two gears are not parallel, the gears contact along a line which is not parallel to their axes. Due to the gear material elasticity, the contact region is an ellipse whose diameters depend on the materials elasticity and the curvatures of the two teeth at point of contact [8]. In practice, the elliptical contact region can be approximated by a line.

For a pair of gears having the specifications listed in table 1, and whose shafts have 1^{o} misalignment, the line of contact was determined. Due to shafts' misalignment, the contact of the teeth does not take place on full face, therefore the meshing stiffness reduces. Figure 8 compares meshing stiffness for ideal case and a case with shaft misalignment.

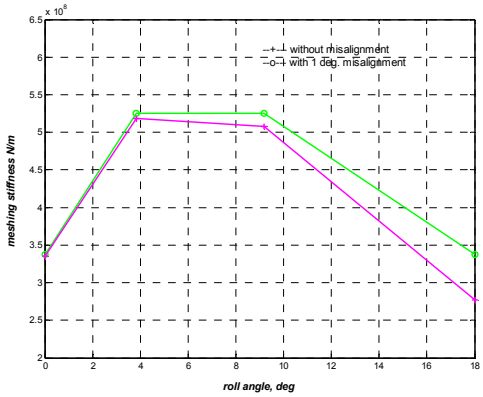

Figure 8- Comparison between ideal contact and a case with shaft misalignment.

CONCLUSIONS

This article presented a new method for calculation of meshing stiffness of gears. The basis of this method is on the assumption of the gear teeth as explicit capacity fields. The stiffness matrix of these fields are determined by assuming virtual interconnected springs on gear surface whose springs constant are determined by three dimensional finite element analysis of the gear teeth. This calculation results in a stiffness matrix for the gear teeth by which the displacement of the teeth along its face for an arbitrary loading can be determined. In addition, the load distribution over the face of the gear for any meshing situation, ideal or non ideal as a result of manufacturing errors, overloading damages, or misalignments can be determined. The results will help engineers in analysis of gear life assessments and catastrophic failure prevention in real life operation.

REFERENCES

1- Dalpiaz, G.; Rivola, A.; Rubini, R.; "Dynamic Modeling of Gear system for Condition Monitoring and diagnostics"; Congress on Technical Diagnostics; 1996.

2- Glodez, Pehan, Flasker; "Experimental results of the Fatigue Crack Growth in a Gear Tooth Root"; Int. J. Fatigue; Vol. 20; No 9; PP. 669-675; 1998.

3- Kuang, J.H.; Yang, Y.T.; "an estimate of Mesh Stiffness and Load Sharing Ratio of a Spur Gear Pair"; International Power Transmission and Gear Conference, vol. 1; ASME 1992; PP 1-9.

4- Pimsarn, M.; Kazerrounian, K; "efficient evaluation of spur gear tooth mesh load using pseudo-interference stiffness estimation method"; Mechanisms and Machine Theory; 2002; vol. 37; PP 769-786.

5- Seireg, A.; Houser, D.R.; "Evaluation of Dynamic Factors for Spur and Helical Gears"; Journal of Engineering for Industry ; Transaction of ASME; vol. 192; 1970; PP 504-515.

6- Shing, T.K.; Tsia, L.W.; Krishnaprasad, P; "An Improved Model for Dynamics of Spur Gear Systems with Backlash Consideration"; ASME DES. ENG. DIV PUBL. DE.; vol. 65; pt. 1; 1993; PP 235-244.

7- Stasa, F.L.; "Applied Finite Element Analysis for Engineers"; 1985.

8- Timoshenko and Goodie, Theory of Elasticity, Mc-Graw Hill, 1970, pp-414- 417.

9- Yesilyurt, Gu and Ball; "Gear tooth stiffness reduction measurement using modal analysis and its use in wear fault severity assessment of spur gears"; NDT & E International 36(2003); PP- 357- 372.